www.amlett.com, www.vbripress.com/aml, DOI: 10.5185/amlett.2015.5827 Published online by the VBRI press in 2015

Characterisation and dielectric property analysis of A-site doped $LaTiO_{3-\delta}$ perovskites synthesised by ball milling method

Bradha Madhavan, Anuradha Ashok*

Nanotech Research Facility, PSG Institute of Advanced Studies, Coimbatore 641 004, India

*Corresponding author. Tel: (+91) 422 4344000; E-mail: anu@psgias.ac.in

Received: 31 January 2015, Revised: 06 March 2015 and Accepted: 06 March 2015

ABSTRACT

The present work highlights a series of perovskites $La_{0.8}A_{0.2}TiO_{3-\delta}$, (where A= Ba, Ca, Sr), which includes a high dielectric constant, a low dielectric loss over a wide temperature, in a frequency range of 30 MHZ. Undoped and A-site doped $LaTiO_{3-\delta}$ (with Ba^{2+}, Sr^{2+} and Ca^{2+}) perovskites were synthesised by solid state reaction method (ball milling). The perovskite phase formation of the milled precursor powders under thermal treatments was investigated by thermogravimetry/differential scanning calorimetry (TG/DSC). Structural analysis of the phase pure sintered pellets revealed an orthorhombic crystal structure for all perovskites. Surface morphology of the sintered pellets exposed the presence of nanosized grains. The oxidation states of La^{3+} and Ti^{3+} ions have been confirmed using X-ray Photoelectron Spectroscopy (XPS). The dielectric spectral analysis reveals that dielectric properties of the perovskites depend on temperature and frequency. Among the dopants Sr is found to be the most effective in increasing the dielectric properties of $LaTiO_{3-\delta}$. This makes it suitable as a high dielectric material for making capacitors operating at higher frequencies.

Keywords: Powders solid state reaction; electron microscopy; dielectric properties; perovskites.

Bradha Madhavan is pursuing her doctorate degree with Prof. Anuradha Ashok in the Department of Nanotech Research Facility, PSG Institute of Advanced Studies, Coimbatore, India. Her research area includes functional materials for energy and catalytic applications.

Anuradha Ashok graduated from the Mangalore University, India in 1995 and received her PhD degree in 2008 from University of Oslo, Norway. She has been doing research in PSG Institute of Advanced Studies, Coimbatore, India since 2009. Her research is primarily focused on the oxide type functional materials for energy applications, Transmission electron microscopy characterisation of materials etc.

Introduction

Perovskite oxides have been given great attention because of their distinctive dielectric, electro optic and other properties. Researchers have exposed that doping with suitable elements in the cationic/anionic sites of these compounds will enhance their properties **[1-3]**. Perovskite-type oxides, particularly with rare earth ions such as La on A site and transition-metal ions on the B site have been subjected to substantial research over the past few decades **[4, 5]**. Significant improvement in their electrical, magnetic, optical, and chemical properties can be achieved by doping in the cationic sites. The achievable applications for these mixed-conducting oxides are broad, extending from components in solid oxide fuel cells (SOFC), oxygen separation membranes, electrochemical reactors, dielectric materials and catalysts **[6]**. Materials with high dielectric permittivity (ε) or ferroelectric materials are of enormous importance as electroceramics for engineering and electronics. Titanate and niobate based perovskites such as $BaTiO_3$ and $LiNbO_3$, have been intensively studied in the past **[7]** for their good dielectric properties. Among such perovskites lanthanum titanates ($LaTiO_{3-\delta}$) are promising materials in various applications because of their ferroelectric, dielectric, electrical conductivity and catalytic properties **[8]**. According to literature, several authors have investigated the A-site doped $La_{1-x}TiO_3$ with different

stoichiometric compositions **[9-13]**. Inaguma et al reported Li doped $La_{2/3}TiO_3$ exhibited the highest ionic conductivity of 10^{-3}(S/cm) at room temperature **[14]**. Ishida & Liebsch reported the electron properties of $LaTiO_3$ **[15]**. Wang et al reported $LaTiO_3$-$Ag_{0.2}$ as a non enzymatic glucose biosensor **[16]**. Xiong et al studied the thermoelectric properties of $La_{2/3}TiO_{2.87}$ **[17].** Balachandran and Error studied the electrical conductivity of polycrystalline $La_2Ti_2O_7$ at elevated temperature **[18]**. The temperature stability coupled with good piezoelectric properties makes $La_2Ti_2O_7$ suitable for possible use as a high-temperature transducer material, while the low-dielectric loss at microwave frequencies make it a candidate material for high-frequency applications **[19]**. A-site doped oxygen deficient lanthanum titanate perovskites $A_{1-x}La_{2x/3}TiO_3$ (A = Ba, Ca, Sr) were prepared and studied for dielectric properties **[20]**. Recently we have prepared $La_{0.8}A_{0.2}TiO_{3-\delta,}$ (where A= Ba, Ca, Sr) and $LaTi_{(1-x)}Sc_xO_{3-\delta}$ (x = 0, 0.2, 0.25, 0.3) by sol-gel method and reported the temperature dependent total conductivity and dielectric properties of A and B site doped $LaTiO_{3-\delta}$ **[21, 22, 23]**. Based on our studies we have reported that Ca doped $LaTiO_{3-\delta}$ showed an enhancement in total conductivity, Sr doped $LaTiO_{3-\delta}$ showed the improved dielectric property. To the best of our knowledge, there is no previous literature available indicating the dielectric properties of $LaTiO_{3-\delta}$, synthesized by ball milling method. By considering the extensive applications of $LaTiO_{3-\delta}$ and advantages of ball milling method of synthesis **[24]** in the present work undoped and A-site doped $LaTiO_{3-\delta}$ were prepared by solid state reaction method. The perovskite is doped with divalent alkaline earth metals Ba, Ca and Sr in trivalent La sites. Substitution of lower valent cations can create more anion vacancies thereby increasing the crystal anisotropy both due to the presence of ions with different radii at the cationic site and defects in the form of vacancies at anionic site. Crystal anisotropy plays an important role in determining the dielectric properties of a material. In this paper we present an overview of the structural and dielectric properties of undoped $LaTiO_{3-\delta}$ and (doped) $La_{0.8}A_{0.2}TiO_{3-\delta}$ (A= Ba, Sr, Ca) perovskites.

Experimental

Materials

High purity (99.9%) chemicals from Merck India Ltd (manufactured at Mumbai) La_2O_3, TiO_2, $BaCO_3$, $CaCO_3$ and $SrCO_3$ were used as precursors for the synthesis of undoped and doped $La_{0.8}A_{0.2}TiO_{3-\delta}$ (A= Ba, Sr, Ca). Emplura Toulene from Merck India Ltd was used as a process controlling agent.

Method

A-site doped (with divalent Ba, Sr and Ca) lanthanum titanate ($LaTiO_{3-\delta}$) nano perovskites were prepared using solid state reaction method (through ball milling). The milling was carried out in a Fritsch pulverisette P5 planetary ball mill at room temperature. Wet milling (with toluene as process control agent) was carried out for 20 h using tungsten carbide milling media at a speed of 300 rpm with ball to powder ratio 10:1. After 20 h milling, the powder was subjected to thermal analysis to identify the temperature range of perovskite oxide phase formation. Based on thermal analysis each powder was calcined separately at 1000 °C for 4 h. All calcined powders were ground into fine powders separately in an agate mortar and then uniaxially pressed into cylindrical pellets of 1.6 mm thickness and 10 mm diameter using hydraulic press by applying a pressure of 180 kg/cm^2. After that pellets were sintered at 1200 °C for 10 h and used for further characterisations and dielectric measurements.

The 20 h milled precursor powder was subjected to thermogravimetry/differential scanning calorimetry (TG/DSC) performed using NETZSCH STA 449F3 simultaneous thermal analyser in static air atmosphere from room temperature to 1100 °C at a heating rate of 10 °C min^{-1} to determine the temperature range of formation of perovskite oxide phase. Structural analysis of the sintered pellets were performed by PHILIPS X-ray Diffractometer with CuKα radiation (λ= 1.540598 Å) with 2θ ranging from 10° to 60° at an acquisition rate of 0.02^o per sec. Unit cell dimensions of the crystal structure were refined by Rietveld (Le-Bail fitting) method using X-pert high score plus program. Microstructure of the sintered pellets was recorded using Carl-Zeiss Auriga scanning electron microscope (SEM) in secondary emission (SE) mode. Dielectric behaviours were studied by impedance measurement using a computer controlled impedance analyser HIOKI 3532 LCR HITESTER in the frequency ranging from 50Hz to 10MHz. For better ohmic contact high temperature curing silver paste was applied on both faces of the pellets.

Results and discussion

Various compositions of the perovskites $La_{0.8}A_{0.2}TiO_{3-\delta}$ where A is Ba, Ca and Sr; and they have been abbreviated as LBTO, LCTO and LSTO respectively, whereas LTO represents the undoped perovskite. This convention has been followed throughout this article.

Thermal analysis

In order to confirm the perovskite phase formation, the 20 h milled powder was subjected to Thermogravimety/ Differential Scanning Calorimetry (TG/DSC). **Fig. 1(a)** shows the TG/DSC curves of the 20 h milled precursors of undoped perovskites (LTO) in static air from room temperature to 1100 °C. As can be seen in the figure, the weight loss occurs in several stages. The first stage in the range between room temperature to 600 °C results due to the removal of moisture, loss of organics and carbon dioxide from the precursors. The second stage between 600 °C – 980 °C is due to the formation of oxides. The third stage in the range of 980 -1100 °C with weight loss is attributed to the oxygen loss and formation of perovskite phase. The DSC curve exposed exothermic thermal effect for all ball milled samples with their respective peaks around 600 °C, 810 °C and 980 °C. These exothermic peaks could be assigned to the oxidation of carbonaceous remains after milling and the formation of crystalline phase. The entire thermal effect was accompanied by the evolution of various gases (such as, CO, CO_2, etc).

Similar thermal behavior was exhibited by all the samples, but only variation is in the third stage as shown in **Fig. 1(b), Fig. 1(c)** and **Fig. 1(d)**. Particularly for LCTO, the formation of oxide phase started at a lower temperature (around 850 °C) possibly because calcium has smaller ionic radius when compared to Ba and Sr. Based on the above results all samples (LTO, LBTO, LCTO, and LSTO) were calcined at 1000 °C for 4 h and subsequently pelletised before using for further characterisations.

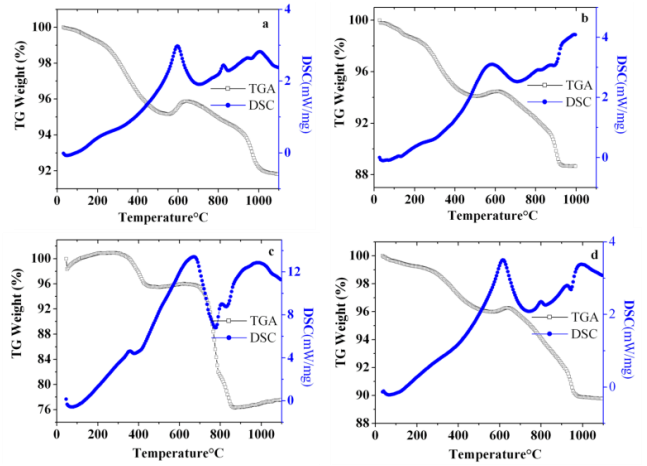

Fig. 1. TG/DSC plots of $La_{0.8}A_{0.2}TiO_{3-\delta}$ (A= Ba, Ca, Sr) 20 h milled precursors (a) LTO, (b) LBTO, (c) LCTO and (d) LSTO.

X-ray diffraction

The powder X-ray diffraction (XRD) patterns of sintered LTO, LBTO, LCTO and LSTO powders (crushed pellets) are shown in **Fig. 2a.** XRD analysis indicates that the perovskites have an orthorhombic crystal structure with different space group and cell dimensions between doped and undoped $LaTiO_{3-\delta}$ as given in **Table 1**.

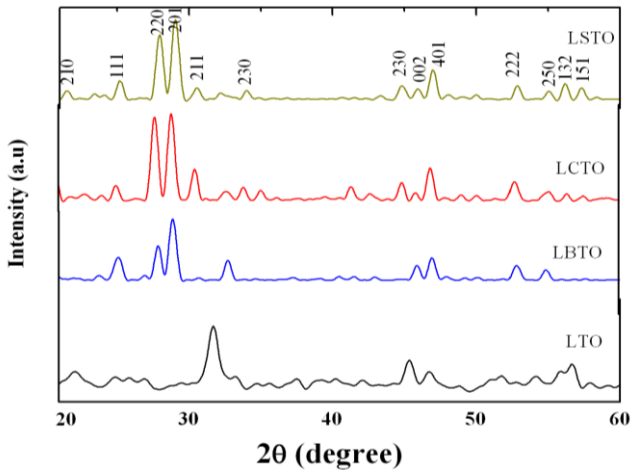

Fig. 2. (a) Powder XRD patterns of sintered $LaTiO_{3-\delta}$ and $La_{0.8}A_{0.2}TiO_{3-\delta}$ (A= Ba, Ca, Sr).

X-ray diffractograms of all doped perovskites have similar peaks. The XRD data of undoped perovskite LTO can be indexed based on an orthorhombic crystal structure with space group Pbnm (62) [PDF#841089 of JCPDS database] as given in **Table 1**. The XRD data of all doped perovskites can be indexed based on an orthorhombic symmetry with a different space group Pna21(33). Cell dimensions of all the doped perovskites calculated using Rietveld analysis of the XRD data based on the space group Pna21(33) [PDF#701690] are given in **Table 1**. Slight changes in the peak positions and intensity are observed in the case of doped perovskites due to the small modifications of cell parameters due to elements having different atomic radii used for A site doping. It can be observed that after doping, the lengths of a and b axes of the orthorhombic unit cells have almost doubled whereas the length of the c-axis has reduced by almost half. This may be due to the ordered substitution of the dopants along certain preferred crystallographic axes/planes of the unit cell. Among the doped perovskites a systematic increase in cell volume is observed with increase in ionic radii of the dopants as shown in **Table 1**.

Table 1. Refined lattice parameters for undoped and doped $La_{0.8}A_{0.2}TiO_{3-\delta}$ (A= Ba, Sr, Ca) perovskites.

Composition	Ionic radii of the doped elements (Å)	Space group and database of JCPDS database	Lattice parameters (Å)			Cell volumes (Å^3)
			a	b	c	
LTO		Pbnm(62) PDF#841089	5.84	5.6	7.7	255.0464
LBTO	1.61	Pna21(33)(PDF#701690)	9.89	9.2	4.7	437.2887
LCTO	1.34	Pna21(33)(PDF#701690)	9.91	9.2	4.9	455.1757
LSTO	1.44	Pna21(33)(PDF#701690)	9.85	9.2	4.9	449.673

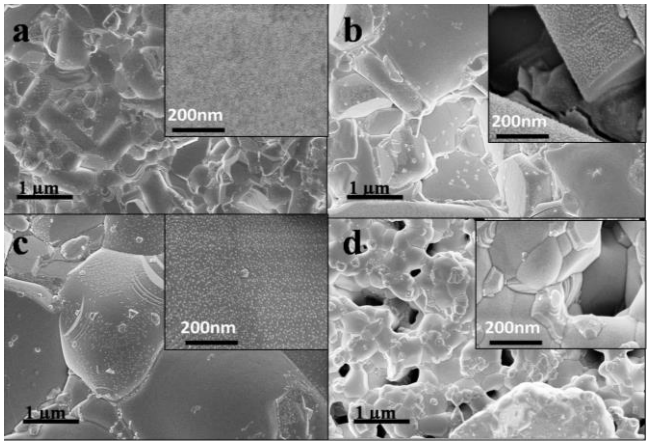

Fig. 3. SEM images of the sintered $LaTiO_{3-\delta}$ and $La_{0.8}A_{0.2}TiO_{3-\delta}$ (A= Ba, Ca, Sr) (a) LTO, (b) LBTO, (c) LCTO and (d) LSTO.

Scanning electron microscopy

The surface morphological features of the sintered pellets were examined through SEM. The micrographs of the sintered pellets are shown in **Fig. 3. Fig. 3(a)** shows morphology of the undoped LTO sample. **Fig. 3(b), (c)** and **(d)** show the micrographs of the doped samples-LBTO, LCTO and LSTO respectively. Insets in each figure show the magnified image of the same sample. Micrographs reveal that pellets are sufficiently sintered and have well defined grains with distinct boundaries. Although the micrographs show a dense structure after doping, closer examination reveals the presence of small voids or pores in the sample. From the inset figures, it can be inferred that

the surface of each particle is composed of smaller particles with irregular morphology indicating grain growth due to high temperature. Prolonged exposure to high temperature may result in agglomeration and fusion of the particles resulting in larger grains, which is apparent from the micro structural images.

X-ray photoelectron spectroscopy

The XPS spectra of La 3d, La 4s, Ti 2p, Ti 2s, Ba 3d, and O 1s regions were analysed for the sintered pellet of LBTO. The respective spectra are shown in **Fig. 4**.

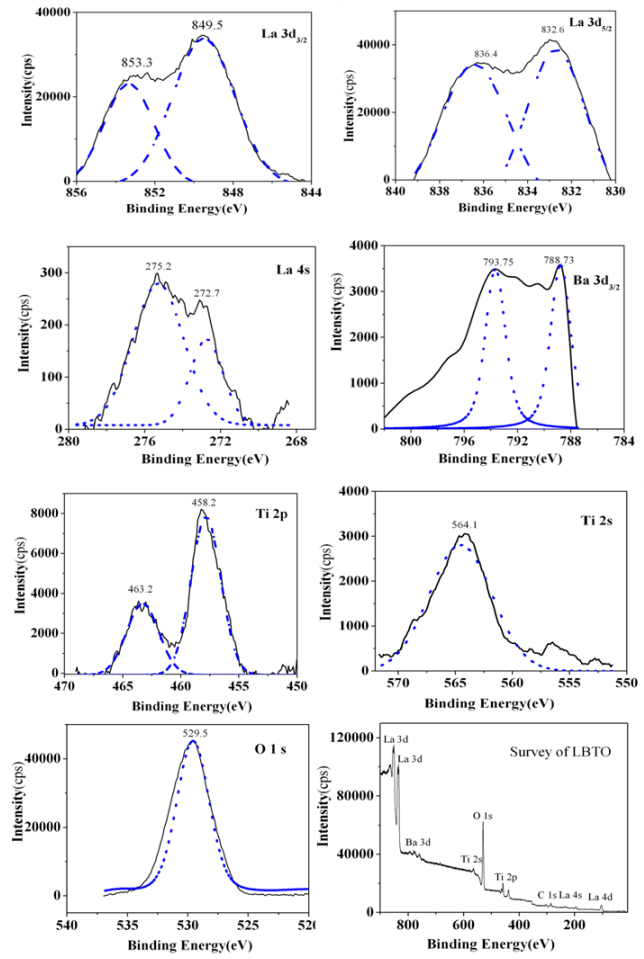

Fig. 4. XPS spectra of the surface of sintered pellet LBTO, depicting the La 3d, La 4s, Ba 3d, Ti 2p, Ti2s, O1s peaks and the survey of LBTO.

The core and the satellite peaks of La $3d_{3/2}$ and La $3d_{5/2}$ components show a clear doublet structure specific for bearing oxides (with peak around ~853.3 eV & 849.5 eV for La $3d_{3/2}$ and 836.4 & 832.6 eV for La $3d_{5/2}$) Energy differences between these peaks are ~3.8 eV. Similarly for La 4s spectrum, the peaks are at 275.2 and 272.7 eV. This is due to the bonding and antibonding states between the $3d^94f^0$ and the $3d^94f^1$ L configurations were L indicates the O 2p hole **[25]**. From the data it is clear that La 3d peaks appeare at 853.3 eV ($3d_{3/2}$) , 836.4 eV ($3d_{5/2}$) and 275.2 eV (4s) which correspond to La^{3+} **[26]**. It can be noticed that the binding energy splitting between the components of both La $3d_{3/2}$ and La $3d_{5/2}$ lines is ~ 4.1 eV in $La_2Ti_2O_7$, $LaNbO_4$ and $Ca_4LaO(BO_3)_3$ crystals and this value is higher than ~3.5 eV in La_2O_3**[27]**. The presence of satellite peak La 3d and La 4s is due to the monopole excitation arising from a change in the screening of the valence electrons upon the removal of a core electron. Similar phenomenon was reported earlier by Miao et al. **[28]** for La^{3+}. In the present system, the Ti 2p located at binding energies 463.2 eV and 458.2 eV respectively indicates the presence of Ti^{3+}. Similarly for Ti 2s the peak was observed at 564.1 eV. This is due to the existence of Ti^{3+}. This type of behaviour was observed for Ti 2p and Ti 2s spectra of TiO_4 and TiO_7 as reported by Rao et al. **[29]**. After sintering at high temperature there is a possible transfomation tendency from Ti^{4+} to Ti^{3+} with a peak shift. This suggests that the Ti ions on the surface of the sample are trivalent. Ba $3d_{3/2}$ spectra shows peaks with binding energy 793.75 eV and 788.73 eV. This can be assigned to the existence of Ba^{2+} ions. The O1s spectrum shows the maximum binding energy at 529.5 eV. When lanthanum and titanium interact with oxygen, valence electrons are transferred from metals to oxygen atoms with variation of the electrical screening in their inner shells. Thus the binding energies of the inner electron metal ions increases together with synchronous decrease in the binding energy of the O1 level of oxygen ions **[30]**. Because of this low tail was observed at higher binding energy side in the O1s peak indicating oxygen defficiency.

Dielectric spectral analysis

From the impedance data imaginary part of impedance, real part of dielectric permittivity, dielectric loss and complex modulus were analysed. **Fig. 5(a)** shows change in imaginary part of impedance Z″ with frequency in undoped sample (LTO) at different temperatures. Z″ increases with frequency, reaches a maximum at a particular frequency, after which it decreases. The maximum impedance value at the peak decreases with increase in temperature indicating a relaxation in the sample. Furthermore, the peak position also shifts towards higher frequency with increase in temperature indicating faster relaxation **[31, 32]**.

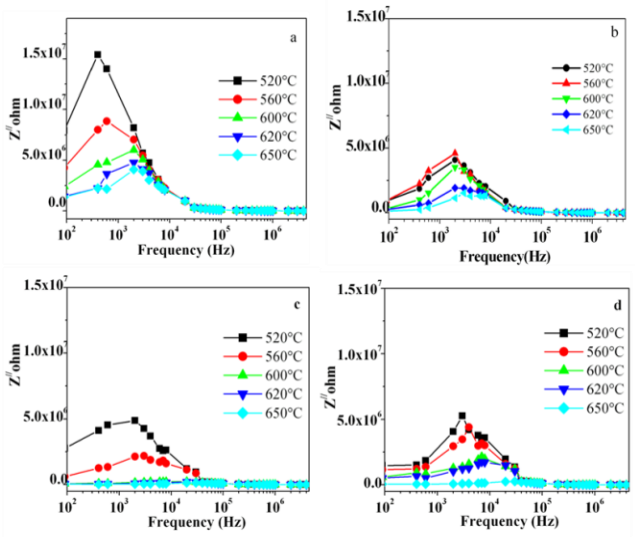

Fig. 5. Variation of imaginary part of impedance of $La_{0.8}A_{0.2}TiO_{3-\delta}$ (A= Ba, Ca, Sr) (a) LTO, (b) LBTO, (c) LCTO and (d) LSTO with frequency at different temperatures.

According to Maxwell Wagner model, a dielectric material consists of many active grains separated by highly resistive boundaries. The voltage applied across the sample drops at grain boundaries and space charge is created **[33]**. The broadening of the peak with increase in temperature confirms the presence of space charges and temperature dependent relaxation process in the sample. There is no significant change in Z″ with frequency in LBTO as shown in **Fig 5(b)**. Furthermore, with increasing temperature the peak broadens significantly and the peak position shifts drastically towards higher frequency for LCTO and LSTO when compared to LTO and LBTO as shown in **Fig. 5(a)** and **Fig. 5(b)**. For LCTO and LSTO at 650°C, Z″ reaches a constant value for all frequencies indicating that the relaxation behavior is related to thermal activation process. It indicates the faster relaxation by release of space charge in LCTO and LSTO as compare to LTO and LBTO.

Variation of imaginary part of the dielectric modulus with frequency at different temperatures is shown in **Fig. 6.** It can be observed that for doped and undoped perovskites, M″ peak shifts towards higher frequency side as the temperature increases. It means the relaxation rate for the process increases with increase in temperature. This representation helps to analyse the apparent polarisation by examination of the magnitude of difference in the peak position by comparing with Z″. The difference in peak position conveys the short range conductivity **[34]**.

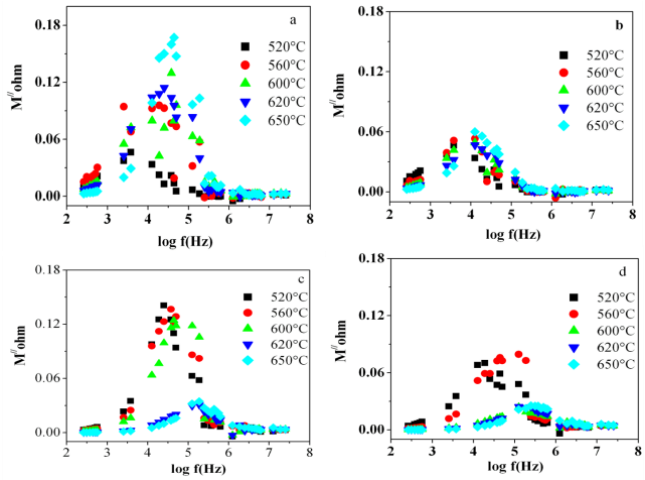

Fig. 6. Variation of imaginary part of dielectric modulus of $La_{0.8}A_{0.2}TiO_{3-\delta}$ (A= Ba, Ca, Sr) (a) LTO, (b) LBTO, (c) LCTO and (d) LSTO with frequency at different temperatures.

Fig. 7 shows the temperature dependent dielectric loss at various frequencies for all the perovskites. For a dielectric material the loss factor is important because it represents the energy loss in a dielectric material. The loss factor appears to depend strongly on the frequency and temperature. The dielectric loss for doped and undoped perovskites decreases with increase in frequency and temperature. At higher frequency all the curves merge together indicating relaxation of the materials. At low temperatures dielectric loss variation is frequency independent. The dielectric loss shows maxima at lower frequencies and minima at higher frequencies at various temperatures because of thermally generated defects in the sample. This is a general behavior of ionic solids where the loss is attributed to both conduction process and space charge polarization which decreases with frequency **[35, 36]**.

Fig. 8a, b, c and d show the variation in the dielectric constant with frequency at different temperatures for LTO, LBTO, LCTO and LSTO respectively. It can be observed that for all perovskites the dielectric constant is the highest at the lowest frequency, decreases with increase in frequency and attain a stable restrictive value at higher frequencies for all temperatures. This is because of dipoles oscillating in an alternating electric field. At very low frequencies ($f << 1/\tau$, τ is the relaxation time), dipoles are stable. At very high frequencies ($f >> 1/\tau$), dipoles can no longer be stable since they cannot follow the alternating electric field. As the frequency increases ($f < 1/\tau$), dipoles begin to decrease following the field, when frequency reaches the characteristic frequency ($f = 1/\tau$), there will be sudden fall in the dielectric constant **[37, 38]**.

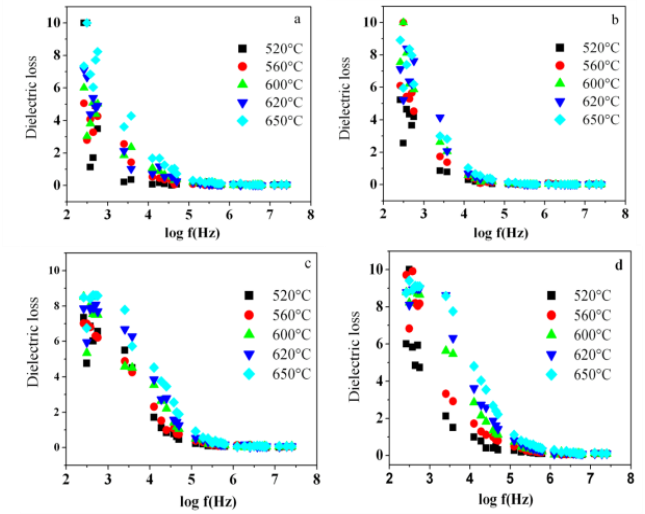

Fig. 7. Variation of dielectric loss of $La_{0.8}A_{0.2}TiO_{3-\delta}$ (A= Ba, Sr, Ca) (a) LTO, (b) LBTO, (c) LCTO and (d) LSTO with frequency at different temperatures.

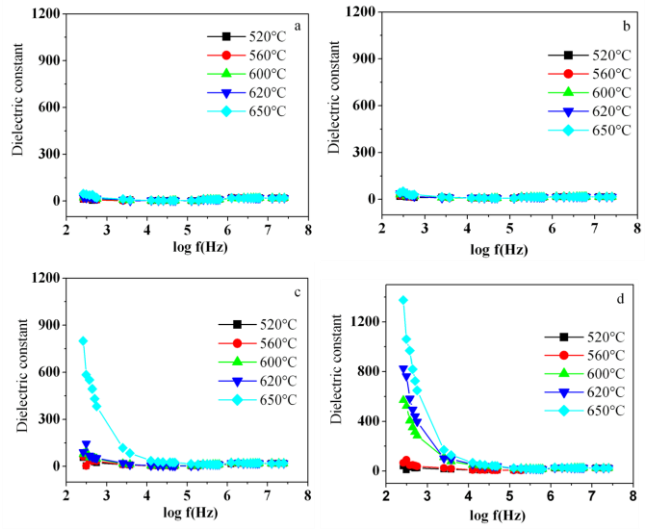

Fig. 8. Variation of dielectric constant of $La_{0.8}A_{0.2}TiO_{3-\delta}$ (A= Ba, Sr, Ca) (a) LTO, (b) LBTO, (c) LCTO and (d) LSTO with frequency at different temperatures.

The observed higher dielectric constant at high temperature at low frequency for all the doped and undoped perovskites might be due to the migration of ions for space charge polarisation. At higher frequencies the space charge polarization vanishes while ionic and electronic polarizations begin to dominate **[39]**. After doping divalent alkaline earth cations in the La site an increase in dielectric constants for LCTO and LSTO (at lower frequencies) was observed. This might be due to the larger extent of crystal anisotropy brought about by the dopants with smaller ionic radii (Sr and Ca, also refer **Table 1**) in larger La (ionic radius 1.36 Å) sites. Whereas substitution of larger Ba^{2+} ions (ionic radius 1.61 Å) in the positions of smaller La^{3+} ions may not result in required crystallographic anisotropy so that it can enhance the dielectric properties. In addition larger Ba ions could also hinder the shorter migration of charges during the formation of space charge polarization. Among Ca and Sr, Sr doped perovskite showed higher dielectric behaviour at all temperatures. Literature indicates that the perovskite $SrTiO_3$ (dielectric constant 300) **[40]** is a better dielectric material than that of $CaTiO_3$ (dielectric constant 160) **[41]**. Based on this observation better dielectric behavior of LSTO may be due to the additional contribution by the Sr ions to the dielectric property when compared to Ca. In addition, larger proportion of grain boundaries (due to smaller grain size, as observed from SEM analysis) in LSTO than in LCTO could enhance space charge polarization. This collectively could contribute for the enhancement of dielectric constant in LSTO.

Conclusion

A-site doped (with Ba^{2+}, Ca^{2+} and Sr^{2+}) and undoped $LaTiO_{3-\delta}$ perovskites were synthesised by ball milling. XRD analysis reveals the formation of single phase orthorhombic perovskite structure. SEM micrographs show well developed grains with almost similar morphology. XPS confirmed that after doping divalent alkaline earth metal cation in the A-site there was no change in the oxidation state of La^{3+} and Ti^{3+}. An enhancement in the dielectric properties was observed after doping in the A site with Sr^{2+} and Ca^{2+}. The dielectric behavior was observed to be predominant at lower frequencies. The results also suggest that ball milling method is appropriate to produce lanthanum titanate perovskites with superior dielectric behavior. From our findings it can be concluded that the materials can be used as ceramic dielectric material having high dielectric constant and low dielectric loss in a frequency range of up to 30 MHz applications such as capacitors.

Acknowledgements

The authors wish to acknowledge UGC-DAE CSR for providing the financial support to carry out this research work, providing facilities for SEM and XPS analysis; Bharathiar University, Coimbatore for extending the facility for impedance measurements and IIT Madras for helping in XRD measurements.

Reference

1. C.D.; Fratello, V.J.; *J. Mater. Res*; **1990**, *5(10)*, 2160. **DOI:** 10.1557/JMR.1990.2041
2. Philips, J.M.; *J. Appl. Phys*; **1996**, *79(4)*, 1829. **DOI:** 10.1063/1.362675
3. Koshy, J.; Kurian, J. ; Jose, R.; John, A.M.;. Sajith, P.K; James, J.; Pai, S.P; Pinto, R; *.Bull. Mater Sci;* **1999**, *22*, 243. **DOI:** 10.1002/adma.200800604
4. Cwik, M.; Lorenz,T; Baier, J.; Müller, R.;. Andr G., Bour,F;. Lichtenberg, F.; Freimuth,A. ; Schmitz, R.; .Hartmann, E. M.; Braden, M.; *Phys. Rev B: Condens. Matter*; **2003**, *68*, 060401. **DOI:** 10.1103/PhysRevB.68.060401
5. Tealdi, C.; Malavasi, L.; Craig. A, Fisher, J.; Saiful Islam, M.; *J. Phys. Chem. B*; **2006**, *110*, 5395. **DOI:** 10.1021/jp057132
6. Meijer, G. I. ; Henggeler, W.; Brown, J.; Becker, O.S.; Bednorz, J. G., Rossel, C.; Watcher, p.; *Phys. Rev. B: Condens. Matter*; **1999**, *59*, 11832 **DOI:** 10.1103/PhysRevB.59.11832
7. Cross L. E. and Newham, R.E.; *J. Am. Chem. Soc.*, **1987**, 111 **DOI:** http://www.ieee-uffc.org/main/history/cross_newnham.pdf
8. Lichtenberg, F.; Herrnberger, A.; Wiedenmann,K.; and Mannhart, J.; *Prog. Solid State Chem;* **2001**, *29*, 1 **DOI:** 10.1016/S0079-6786(01)00002-4
9. MacChesney, J.B.;.Sauer, H.A; *J. Am. Ceram. Soc;*. **1962**, *45* 416. **DOI:** 10.1111/j.1151-2916.1962.tb11185.x/abstract
10. Mac Earchern, M.J. ; Dabkowska, H.; Garrett, J.D.; Amow, G.; Gong W; Liu,G; Greedan; J.E; *Chem. Mater.*; *1994*, *6*, 2092 **DOI:** 10.1021/cm00047a032
11. MacChesney, J.B.; Gallagher, P.K., Dimarcello, F.V; *.J. Am. Ceram Soc;*. **1963**, *46*, 197 **DOI:** 10.1111/j.1151-2916.1963.tb19771.x/full
12. Ali, R.; Yashima, M.; Tanaka, M. ;. Yoshioka, H; Mori, T. ; Sasaki, S.J. ; *Solid State Chem*; **2002**, *164*, 51. **DOI:** 10.1006/jssc.2001.9447
13. Vashook , V., Vasylechko L., Knapp, M.;. Ullmann, H; Guth, U.; *J.Alloy Compd;* **2003**, *354*, 13. **DOI:** 10.1016 / S0925-8388(02)01345-2
14. Inaguma, Y; Liquan, C; Itoh, M; *Solid State Commun*, **1993**, *86*, 689. **DOI:** 10.1016/0038-1098(93)90841-A
15. Ishida, H ; Liebsch, A; *'Physical Review B.,* **2008**, *77*, 115 **DOI:** http://dx.doi.org/10.1103/PhysRevB.77.115350
16. Wang, YZ,; Zhong, H,; Li, XM,; Jia, FF,;Shi, YX,; Zhang, WG,; Cheng, ZP,; Zhang, LL,; Wang, JK; **2013**, *Biosens. Bioelectron. 48*, 56. **DOI:** 10.1016/j.bios.2013.03.081
17. Xiong, X; Tian,R; Lin, X; Chu, D; Li S, *RSC Adv.*, **2015**, *5*, 1473 **DOI:** 10.1039/c4ra13945c
18. Balachandran, U ; Error, NG ; J Less Common Met, **1982**, *85*, 111. **DOI:** 10.1111/j.1151-2916.1981.tb10288.x/abstract
19. Yamamoto, JK,; Bhalla, AS;, J. Appl. Phys.', **1991**; 70, *8*, 4469. **DOI:** 10.1063/1.349078
20. Tien, TY ; Cross, LE; *Jpn. J. Appl. Phys;*. **1967**, *6*, 459 **DOI:**10.1143/JJAP.6.459
21. Bradha, M,; Hussain, S,; SujayChakravarty,; Amarendra, G; Anuradha Ashok, *Ionics*, **2014**, *20*, 1343. **DOI:**10.1007/s11581-014-1216-y
22. Bradha, M. ; Anuradha Ashok, *J. Sol gel Science and Technol*. **2015,** *73*, 1-8 **DOI:** 10.1007/s10971-014-3486-2
23. Bradha, M,; Hussain, S,; SujayChakravarty,; Amarendra, G,; Anuradha Ashok;, *J.Alloy Compd;* **2015**, *626*, 245. **DOI:** 10.1016/j.jallcom.2014.12.033
24. Praveen K. B,; Sreenivasalu. G;, Kumar, H. H.; Kharat, D. K. Balasubramaniam, M.; Murthy, B. S.*; Mater. Chem. Phys*, **2009**, *117*, 338-342 **DOI:** 10.1016/j.matchemphys.2009.06.032
25. Nelson, A J,; Adams, J J; Schaffers, K,; *J. Appl. Phys;*. **2003**, *94*, 7493 **DOI:** 10.1063/1.1627955
26. Teterin Yu, A,; Baev, A. S,; X-Ray Photoelectron Spectroscopy of Lanthanide Compounds (Moscow: CNII atom in form) (in Russian) **1987**.
27. Teterin Yu, A,; Teterin A Yu ,. *Chem. Rev*, **2002,** *71*, 347. **DOI:** 10.1070/RC2002v071n05ABEH000717
28. Miao, J.P.; Li, L.P.; Liu, H.J. ; Xu, D.P. ;.Lu, Z ; Song, YB ; Su,WH; Zheng,YG,; *Mater let*, **2000**, *42*, 1. **DOI:** 10.1016/S0167-577X(99)00149-4
29. Rao, CNR,; Sarma, D.D*; J. Solid State Chem*.**1982**, *45*, 14. **DOI:** 10.1016/0022-4596(82)90288-2

30. Rojas, M. L. ;. Fierro, J. L. G ; *J. Solid State Chem*, **1990,** *89*, 299.
31. **DOI:** 10.1016/0022-4596(90)90271-X
32. Shukla, A.;. Choudary, R.N.P,;.Thakur, A.K; Pradhan, D.K. *Physicia B*, **2010**, *40*, 599
DOI: 10.1016/j.physb.2009.08.075
33. Sen, S.;. Mishra, S.K S. ; Sagar Palit, ; Das, S.K.; Tarafdar, A. *J.Alloy Compd;* **2008**, *453*, 395.
DOI: 10.1016/j.jallcom.2006.11.126
34. Koops, C.; *Phys.Rev* ; **1951**, *83*, 121.
DOI: 10.1103/PhysRev.83.121
35. Bajpai, P.K; Singh, K.N.; *Physica B* **2011**, *406*, 1226.
DOI: 10.1016/j.physb.2010.12.069
36. 36. Maccallum, R.J; Vicent, C.A.; *Polymer Electrolyte Reviews-1*', **1987.**
37. Kyritsis,A; Pissis,P,; .Grammatikakis, J;, *J.Polym. Sci. Part, B:***1995,** *33*, 12.
DOI: 1737 10.1002/polb.1995.090331205
38. Ved Prakash, Choudhary, S.N.; Sinha, T.P.; *Physica B*, **2008**, 403.
DOI: 103 10.1016/j.physb.2007.08.015
39. Tripathi, R.;. Kumar, A; Bharti, C;. Sinha, T. P, Curr.Applied Physics, **2010,** *676*, 10.
DOI: 10.1016/j.cap.2009.08.015
40. Jonscher, A.K; *Nature* **1977**, *267*, 673.
DOI: 10.1038/267673a0
41. Han,J,; Wan, F,; Zhu, Z,; Zhang, W,; *App. Phy.Letters*, **2007**, *90*, 031104.
DOI: 10.1063/1.2431448
42. Pashkin, A.; Kamba, S; Berta, M,; Petzelt, J; Csete de Gy¨orgyfalva, G D C,; Zheng, H; Bagshaw H.; Reaney, I. M.,; *J. Phys. D: Appl. Phys*. **2005**, *38*, 741.
DOI: 10.1088/0022-3727/38/5/012